JOURNAL OF CATALYSIS 72, 37–50 (1981)

Mössbauer Spectroscopy of Supported Fe–Co Alloy Catalysts for Fischer–Tropsch Synthesis

R. M. STANFIELD AND W. N. DELGASS

School of Chemical Engineering, Purdue University, West Lafayette, Indiana 47907

Received July 14, 1980; revised July 21, 1981

The effects of pretreatment, reduction, reoxidation, and CO hydrogenation at 1 atm pressure on silica-supported Fe–Co catalysts are reported. Air drying the catalysts after incipient wetness preparation produced larger metallic crystallites than vacuum drying. Upon reduction the Fe and Co interact and form bimetallic clusters on SiO_2, as evidenced by the increased reducibility of the Fe and the variation of the magnetic hyperfine field of the Mössbauer spectra as a function Co loading. Disorder in the local Fe–Co environment within the particles is indicated in the Mössbauer effect by large linewidths and slight deviations from the expected values of the hyperfine field. Materials with up to 10 at.% Co in Fe (10% by weight total metal loading) form carbides during reaction, but at a slower rate than Fe alone on SiO_2. At higher than 25 at.% Co concentration in iron, little change occurs when the reduced state is exposed to a 3.2 H_2-to-CO mole ratio syngas at 523°K, atmospheric pressure, and differential conversion.

INTRODUCTION

Iron and cobalt are historically the classical Fischer–Tropsch synthesis catalysts. In early tests with precipitated and fused catalysts (*1*, *2*), it was determined that Fe produces more branched hydrocarbons and tends to form more olefins and oxygenated products compared to Co. Phase changes during reaction were also found to be significantly different for these metals. Reduced Fe catalysts form carbides and oxides during reaction and precarbided catalysts show enhanced activity with similar selectivities. In contrast, Co catalysts show little tendency to form oxides or carbides and precarbiding significantly lowers the activity. The abilities of both metals to hydrogenate ethylene and propylene, however, are very similar (*3*, *4*), and for both catalysts, life and activity were found to be enhanced by medium-pressure operation (5–15 atm).

Recent work by Vannice, done at atmospheric pressure and differential conversion with 3 H_2/CO syngas on silica-supported catalysts, shows that Co is more methane selective (~72% at 493°K) than Fe (~60% at 520°K) (*5*, *6*). He also demonstrated, using turnover numbers based on CO chemisorption, that Co/SiO_2 is about an order of magnitude more active than Fe/SiO_2 for methanation. This finding is in contrast to results for alumina-supported metals in which Fe was found to be more active than Co. The reasons for the difference are not completely understood, but Vannice has postulated incomplete reduction of alumina-supported Co as a cause.

Along with its difference in hydrocarbon selectivity, Co tends to favor H_2O formation as a by-product of the synthesis, whereas Fe favors CO_2 (*1*, *7–9*). However, when lower gas flow or higher temperature is employed, the Co catalysts can give sizable yields of CO_2 (*1*).

Other contrasts between these metals are apparent from recent surface science studies of well-defined single crystals, which show differences in CO dissociation abilities of these two materials. Low-Miller-index surfaces of Fe single crystals dissociate substantial amounts of CO at 300°K and exhibit enhanced dissociation with increasing temperature (*10–13*). In turn, Co is less active for CO dissociation.

0021-9517/81/110037-14$02.00/0

The basal plane is inactive for dissociation and the $(10\bar{1}2)$ plane adsorbs CO associatively at room temperature; dissociatively only after heating (*14, 15*).

In terms of physical properties, Fe and Co have many similarities. They have very similar atomic radii (1.165 and 1.162 Å, respectively), percentage *d* character (39.7 and 39.5), and equivalent metallic-state valences, based on the work of Pauling (*16, 17*). Details of the phase diagram still need further substantiation, but it is known that Fe and Co form bcc substitutional solid solutions below 70% Co and 1173°K (*18*). Ordered structures occur at $FeCo_3$, FeCo, and Fe_3Co (*19*).

Little information has been published concerning Fischer–Tropsch synthesis using the Fe/Co catalytic system. Recently, however, Wise and co-workers have reported a maximum in selectivity for C_2 plus C_3 hydrocarbons at the 50% Co bulk catalyst composition for unsupported, precipitated catalysts (*20*). Additionally, these authors have theoretically predicted and experimentally measured by Auger electron spectroscopy surface enrichment of Fe in this alloy (*21*). In our laboratory, results obtained using a differential plug flow reactor show that unsupported Fe–Co powders have selectivities which are not linearly related to bulk composition but show a dominant influence of iron (*22*).

The Fe/Co catalytic system lends itself particularly well to study with Mössbauer spectroscopy since ^{57}Fe is the prime Mössbauer probe atom and this spectroscopy has been applied to the study of catalytic systems very successfully (*23, 24*). Briefly, the attributes of Mössbauer spectroscopy are that examination of the spectrum of an Fe-containing catalyst yields such information as the oxidation state of the Fe, the existence of bimetallic clusters, and in some cases a rough estimate of particle size of the Fe-containing crystallites. Although there is a void in the literature concerning Mössbauer investigations of Fe/Co catalysts, studies of the bulk alloy report changes in the magnetic hyperfine field and linewidths with composition and ordering (*25–27*). These results will be discussed in comparison to the findings of this research later in the paper.

From the above discussion it is apparent that Fe and Co have many similarities with respect to their ability to perform the Fischer–Tropsch synthesis and some of their metallic properties. However, significant catalytic and physical differences are also apparent. In this work we have investigated the chemistry of the $Fe–Co/SiO_2$ system and the Fischer–Tropsch synthesis behavior of well-characterized supported Fe–Co catalysts. We report here the effects of reduction, reoxidation, and CO hydrogenation on the chemical nature of the catalysts. Conditions needed for alloy formation are also discussed. Subsequent papers will report chemical kinetics, details of the effects of different pretreatments and support pore structures, and the dynamic response of the catalysts to reaction mixtures.

EXPERIMENTAL METHODS

The Fe- and Fe/Co-on-silica catalysts used in this study were prepared via the incipient wetness technique. An aqueous solution of the proper ratio of iron and cobalt nitrate salts was added to dry Cab-o-Sil EH5 silica (~390 m^2/g) dropwise until the porous powder appeared wet. Impregnated samples were then left to air dry at room temperature for a minimum of 2 weeks. Typically, a sample of 0.1 to 0.3 g of catalyst powder was then pressed at 8000 psi into a 1.7-cm-diameter, self-supporting wafer and heated to decompose the nitrate salts. Two methods of heat treatment were employed to remove excess water and decompose the nitrate salts. The first method, consisted of vacuum drying the catalyst wafer at a pressure of ~126 Torr. Slow vacuum drying, accomplished by raising the temperature to 413°K in five 20–25°K increments spread equally over 8 hr and then holding at 413°K for an additional 24 hr, and fast vacuum drying, accomplished by in-

serting the sample into the 413°K oven, pumping to ~126 Torr and holding for 24 hr, give indistinguishable catalysts. The second method consisted of drying the samples in air by incrementing the temperature by the same schedule as that for slow vacuum drying.

All catalyst compositions are reported on a dry, reduced basis as xFeyCo/SiO_2, where x and y are the weight percentages of the Fe and Co, respectively. All catalysts studied had a total metal loading ($x + y$) of 10 wt%. Due to the longer counting times required for the Mössbauer spectra at lower Fe loadings, the highest Co loading studied was 3.87Fe6.13Co/SiO_2.

The Austin Science Associates constant-acceleration Mössbauer spectrometer and high-temperature absorber cell used in this work have been described elsewhere (*28, 29*). The source was 50 mCi of ^{57}Co diffused into a Rh matrix (supplied by Amersham Corp.), but all Mössbauer spectra presented here have zero isomer shift referenced to a 25-μm NBS Fe foil. A multipurpose gas-handling system (described in Ref. (*28*)) allows evacuation of the absorber cell to $<1 \times 10^{-5}$ Torr and flow at 1 atm of H_2, O_2, He, or a 3.2 H_2/CO synthesis gas. All gases were UHP grade from Matheson with the H_2 and synthesis gas being further purified by passage through an Engelhard Deoxo 10 ft^3/hr capacity oxygen–hydrogen catalytic purifier and a subsequent bed of 5A and 13X molecular sieves to remove water.

The Mössbauer data were computer fitted to Lorentzian lineshapes by a variable-metric minimization program (*30*). The fitting routine allowed easy application of simple linear constraints of dips, widths, and relative positions of the fitted peaks. These constraints were only applied when two or more peaks in the spectra overlapped and only when they could be justified physically. For example, the ferrous species found in the reduced spectra was fit with two doublets if a significant relative area could be attributed to this material, otherwise only one doublet or no peaks were fit to this material. When fitting two doublets, however, it was found that constraining the widths and dips of the outer doublets to be equal, but requiring only equal widths of the inner doublet, consistently gave reasonable and reproducible estimates of the fitted parameters for these peaks. As many as three, six-line, magnetically split Fe sites were present in the Mössbauer spectra of carburized catalysts after reaction, however. The fitting of these spectra was achieved by constraining the peak dips and linewidths to be equal for companion peaks in a sextet, i.e., peaks 1 and 6, 2 and 5, 3 and 4. If the intensity of the magnetically split site was low, additional constraints, such as forcing the ratio of peak dips to be 3 : 2 : 1 and the linewidths to all be equal for the six-line set, were imposed. The solid lines drawn through the spectra in this paper are calculated from the fitted parameters.

Two X-ray diffractometers supplied the diffraction patterns for the catalyst pellets. The first was a General Electric model XJD-5 and the second was a Siemens type M 386-x-A9 with a PDP-11/05 computer controller. Both used Cu$K\alpha$ radiation. Iron and iron alloy foils were used to correct for instrumental broadening. Reduced samples were passivated by flowing UHP He over them at room temperature with gradual admittance of UHP O_2 over a 3- to 4-hr period until the gas stream contained approximately 21% O_2. The passivation sequence was as follows. After He flowed over the reduced catalyst for 20 min at 240 cm^3/min, pulses of O_2 at ~50 cm^3/min were admitted to the He stream at 20-min intervals. The pulse durations were 1 s, 1 s, 2 s, 2 s. The O_2 flow rate was then increased to 64 cm^3/min and pulsed into the He stream at 20-min intervals for time intervals of 3 s, 3 s, 5 s, 10 s, and 20 min. The last prolonged pulse of O_2 had 21% O_2 in the gas phase over the catalyst.

The amount of oxide appearing in the Mössbauer spectrum of the passivated cat-

alyst depended on the average crystallite size of the iron phase. For 8-nm particles ~30% of the spectral area corresponded to oxidized iron, whereas 2-nm particles showed less than 5% of the spectral area as oxidized iron after passivation. In the thin absorber limit, the relative spectral area is proportional to the concentration of a given species times its recoil-free fraction (*31*). Large differences on recoil-free fraction should be indicated by a significant change in total spectral area with chemical treatment. Throughout these experiments total areas did not change by more than 4%. Thus, for purposes of estimation of relative amounts of various iron species, we assume that the recoil-free fractions of all species are approximately equal. Using this assumption to calculate the thickness of the passivated oxide skin over the iron core, we find that the passivation procedure should cause an 11% underestimate of particle diameter in XRD of 8-nm crystallites and a 2% underestimate for the 21-nm ones. This error is small compared to the usual error of ~20% often encountered in XRD line-broadening experiments and has, therefore, been neglected in this work.

During Fischer–Tropsch synthesis reactions, a Hewlett–Packard model 5834A reporting gas chromatograph, equipped with thermal conductivity and flame ionization detectors, was used to analyze the hydrocarbon products in the effluent gas from the Mössbauer cell. This device had microprocessor control for temperature programming of a Chromosorb 102 column and gave good separation and sensitivity for C_1 through C_5 paraffins and olefins. The carrier gas was He. Absolute calibration was obtained prior to each run by analysis of a certified standard calibration gas mixture prepared by Matheson Corporation.

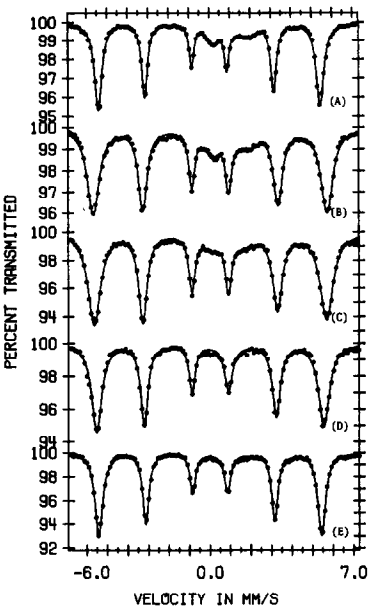

FIG. 1. Room-temperature Mössbauer spectra of vacuum-dried catalysts after reduction in flowing H_2 at 723°K for 8 hr. (A) 9.47Fe0.53Co/SiO_2; (B) 7.4Fe 2.6Co/SiO_2; (C) 5.87Fe4.13Co/SiO_2; (D) 4.87Fe5.13 Co/SiO_2; (E) 3.87Fe6.13Co/SiO_2.

RESULTS AND DISCUSSION

Reduced Catalysts

After drying, the samples were placed in the absorber cell and evacuated to 10^{-5} Torr to remove any excess water adsorbed during transfer to the cell and to facilitate a vacuum leak check of the gas flow system. For all samples, Mössbauer spectra taken during this procedure consisted of a broad doublet near 0.3 mm/s, characteristic of Fe^{3+}. The catalysts were then reduced in flowing hydrogen by heating the samples from room temperature to 723°K over approximately ½ hr and holding this temperature for 8 hr. Mössbauer spectra were taken in hydrogen after the samples cooled to room temperature. Spectra for the vacuum-pretreated catalysts are given in Fig. 1. The estimated average particle size as determined by XRD after reduction and passivation, and the parameters of the computer fits are given in Table 1. Figure 2 gives the spectra for the reduced, air-dried catalysts while Table 2 summarizes the quantitative XRD and Mössbauer analysis of these catalysts.

Many trends are apparent in Figs. 1 and 2. All of the reduced catalysts show the six

TABLE 1

Mössbauer Parameters and Estimated Particle Sizes for Reduced Samples, Fig. 1.

Spectrum: / Catalyst:	A 9.47Fe0.53Co/SiO_2	B 7.4Fe2.6Co/SiO_2	C 5.87Fe4.13Co/SiO_2	D 4.87Fe5.13Co/SiO_2	E 3.87Fe6.13Co/SiO_2
Isomer shift (mm/s)					
Alloy	0.01	0.04	0.04	0.03	0.02
Fe^{2+}	1.02	1.06	0.92		
Fe^{2+*}[a]	0.86	0.82			
Quadrupole splitting (mm/s)					
Fe^{2+}	1.92	1.99	1.65		
Fe^{2+*}	1.02	1.22			
Magnetic field (kOe)					
Alloy	336.5	354.7	352.3	344.5	337.7
Average outer ferromagnetic linewidth (mm/s)	0.45	0.70	0.76	0.60	0.45
Fraction of spectral area magnetically split	0.85	0.87	0.92	1.00	1.00
Estimated particle size–XRD (nm)	8	8	8	9	11

[a] Assigned to surface-active iron oxide.

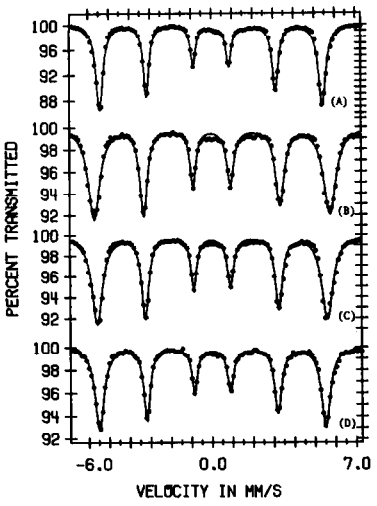

FIG. 2. Room-temperature Mössbauer spectra of air-dried catalysts after reduction in flowing H_2 at 723°K for 8 hr. (A) 9.47Fe0.53Co/SiO_2; (B) 5.87Fe 4.13Co/SiO_2; (C) 4.87Fe5.13Co/SiO_2; (D) 3.87Fe6.13 Co/SiO_2.

main peaks characteristic of ferromagnetic Fe. For the vacuum-dried catalysts at the high Fe loadings (Fig. 1), two broad peaks attributable to unreduced Fe are also present at ~0.2 and 2.0 mm/s. Fitting of the spectra was improved if these peaks were assigned to two doublets, corresponding to low-coordination-number (isomer shift (IS) ~0.8 mm/s, quadrupole splitting (QS) ~1.0 mm/s) and high-coordination-number (IS ~ 1.0 mm/s, QS ~ 1.9 mm/s) Fe^{2+} species. Similar assignments have been made previously for Fe-on-silica supported catalysts (*32*). In the present study, both unreduced phases probably arise from iron which is close to or in direct contact with the oxidic support. The bulk species is shielded from adsorbing gases by either reduced or no-reduced surface-active iron depending on the crystallite size of the iron phase. The surface-active species can interact with adsorbing gases such as NH_3, as has been evidenced by changes in the quadrupole splitting in the Mössbauer spectra (*32*). No unreduced iron was detectable in the 4.87Fe5.13Co/SiO_2 and 3.87Fe6.13Co/SiO_2 catalysts. This enhancement of reducibility appears to be the result of the presence of Co which has been known to reduce more easily than Fe in Fischer–Tropsch catalysts (*1*). Enhanced reducibility of the Fe in bimetallic clusters has been reported for Fe–Pt (*33*), Fe–Pd (*34*), Fe–Ru (*35*), and Fe–Rh (*36*) catalytic systems. In all of these cases, the Fe was reported to be in intimate contact with the other metals.

After the air-drying pretreatment and subsequent reduction (Fig. 2), practically all the Fe was in the reduced state even at the high Fe/Co ratios. There is less interac-

TABLE 2

Mössbauer Parameters and Estimated Particle Sizes for Reduced Catalysts, Fig. 2

Spectrum:	A	B	C	D
Catalyst:	9.47Fe0.53Co/SiO_2	5.87Fe4.13Co/SiO_2	4.87Fe5.13Co/SiO_2	3.87Fe6.13Co/SiO_2
Isomer shift (mm/s)				
Alloy	0.01	0.03	0.02	0.02
Magnetic field (kOe)				
Alloy	336.6	356.6	347.6	342.4
Average outer ferromagnetic linewidth (mm/s)	0.44	0.70	0.65	0.53
Estimated particle size–XRD (nm)	21	16	20	14

tion between the support and the crystallites in these catalysts because a smaller percentage of metal is in contact with the oxidic support at the larger particle sizes.

Figures 1 and 2 reveal another interesting change with composition. The magnetic hyperfine field, which is proportional to the distance between the outside two peaks, goes through a maximum and then declines with increasing Co loading. The solid line in Fig. 3A is the magnetic field recorded by Johnson *et al.* for bulk alloys (*27*). These results on bulk alloys have been confirmed by later studies (*23, 26*) and in our laboratory at the 25 and 40% Co composition. On the basis of conversion from Mössbauer splitting to internal magnetic field based on the assignment of the value 330 kOe for iron foil, the points corresponding to the magnetic fields of the supported catalysts in this study are also shown in Fig. 3A. The trend for the catalyst samples is the same as that of the bulk alloys. This empirical agreement between the catalyst and bulk data is positive proof that the Fe and Co are in intimate contact and that bimetallic alloy particles have formed.

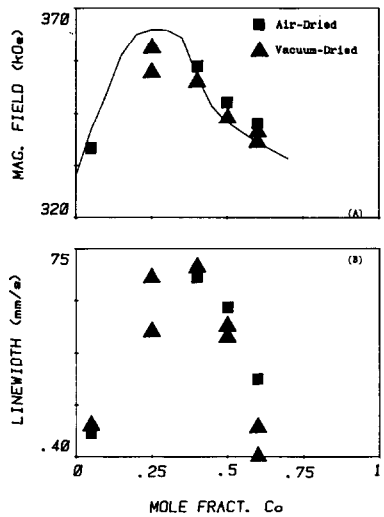

FIG. 3. (A) Magnetic fields vs Co content. The solid curve is the reported bulk Fe–Co alloy data after Johnson *et al.* (*27*). (B) Average outer peak linewidths of ferromagnetic material vs Co content.

The exact values for the magnetic fields of the catalyst do, however, show some deviation from the bulk values. They are low at 5% and especially 25% Co and are generally high at higher Co concentrations. It is not uncommon for small crystallites, such as those found on supported catalysts, to exhibit reduced magnetic splittings as compared to bulk forms (*36, 37*), but increased magnetic splittings cannot be explained by particle size effects. Two alternative explanations are possible. The first is that the expected overall composition was not actually achieved. Atomic absorption studies at the $7.4Fe2.6Co/SiO_2$ composition have confirmed, however, that the correct loading was achieved with this preparation. Since a known quantity of metal is laid down on the support and no volatile hydrates or oxides of Fe or Co exist, we assume that all overall compositions are correct. The second explanation is inhomogeneity of the samples caused by changes in the local concentration of the two components in the metal crystallites. Although not so clear for the 5% Co composition, it is easily seen that any inhomogeneity or disorder at the 25% Co composition would decrease the magnetic field from the maximum value. Because of the curvature of the magnetic field versus composition line at the higher Co loadings, the magnetic field should increase with local atomic disorder or local composition variations in this region. Such increases in field have indeed been reported for disordered 40 to 60% Co bulk alloys prepared by rapid quenching from a temperature above the order–disorder transition (*25, 26*).

Additional evidence that inhomogeneity or local disorder is present in the catalyst samples can be seen by examining the variation of the outer-peak linewidths. The linewidth of a Mössbauer spectrum is a measure of the diversity of sites that are present for the iron atoms in the sample. A variety of local environments, i.e., a distribution in the number of Co atoms in the first coordination sphere of Fe, gives a distribution of

internal magnetic fields. The sum of the slightly different fields yields a broadened spectrum.

Figure 3B is a plot of the average outside-peak linewidths of the catalyst samples versus Co composition. The data show a definite trend with a maximum at approximately 40 at.% Co. The linewidths of ordered bulk alloys show no change with composition, but increases in the linewidths by about 50% were reported at the 50% Co composition for the disordered alloys (*26*). Thus, the increased peak widths for the catalyst samples are consistent with the presence of disorder in the alloys. To check whether the variation in linewidth could be attributed to concentration gradients of the metals across the wafers rather than local disorder within the crystallites, a 40% Co catalyst (5.87Fe4.13Co/SiO_2) was annealed in H_2 at 823°K for 24 hr in hydrogen. XRD indicated no measurable particle size change after the annealing, but the Mössbauer linewidth decreased by 15% while the internal magnetic field was essentially unchanged at 351.4 kOe compared to 351.7 kOe before annealing. This reduction in linewidth must be caused by local ordering within the crystallites themselves since transport of atoms from the extremities of the wafer to the interior is unlikely. Some contribution to the line broadening by composition variation from crystallite to crystallite is still possible, but the annealing experiment shows that local disorder also plays an important role.

Used Catalysts

After reduction the catalysts were flushed with He and heated to 523°K in the absorber cell. Syngas with a 3.2 H_2/CO mole ratio and flow rates from 20 to 100 cm^3/min was then passed over the sample at atmospheric pressure for 6 hr at 523°K. In all cases conversions were less than 10%. After reaction, the system was cooled to room temperature in flowing He and Mössbauer spectra were taken.

Figure 4 shows spectra for the vacuum-dried catalysts. Computer fits of the spectra for 4.87Fe5.13Co/SiO_2 and higher-Co-content catalysts showed only slight changes after reaction as can be seen by comparing Tables 1 and 3. Reduced, air-dried catalysts in this composition region were also unchanged by reaction. Spectra of catalysts with a higher Fe/Co ratio, however, show clear evidence for carbide formation as in Fig. 4A for the 9.47Fe0.53Co/SiO_2 vacuum-dried sample. Many stable and intermediate iron carbide phases are discussed in the literature (*38–44*). The most important phases likely under our experimental condition are ϵ', ϵ, η, and χ (or Hagg). The familiar θ or cementite phase is formed at higher temperatures. A recent paper by Niemantsverdriet *et al.* (*45*) shows that the X-ray diffraction pattern of Barton and Gale (*46*), previously assigned to ϵ carbide, corresponds to the phase which has been assigned as ϵ' on the basis of its Mössbauer spectrum (*39*). It is apparent from this and other literature that differentiation of the hexagonal and pseudo-hexagonal phases (ϵ', ϵ, and η) is very difficult. Since such

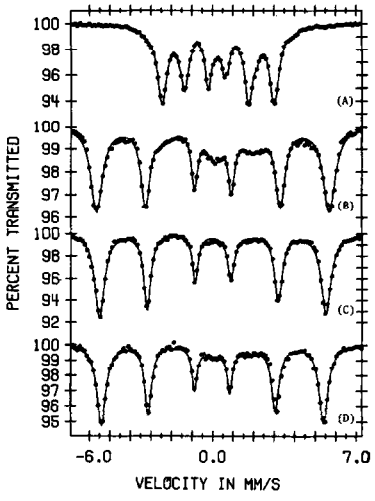

FIG. 4. Room-temperature Mössbauer spectra of vacuum-dried catalysts after 6 hr of reaction at 523°K in flowing 3.2 H_2/CO synthesis gas. (A) 9.47Fe 0.53Co/SiO_2; (B) 7.4Fe2.6Co/SiO_2; (C) 4.87Fe 5.13Co/SiO_2; (D) 3.87Fe6.13Co/SiO_2.

TABLE 3

Mössbauer Parameters for Used Catalysts, Fig. 4

Spectrum: Catalyst:	A 9.47Fe0.53Co/SiO_2	B 7.4Fe2.6Co/SiO_2	C 4.87Fe5.13Co/SiO_2	D 3.87Fe6.13Co/SiO_2
Isomer shift (mm/s)[a]				
Alloy		0.03	0.02	0.02
Fe^{2+}	1.02	1.06		0.93
Fe^{2+}*	0.86	0.82		
I	0.28	0.28		
II	0.37			
III	0.28			
Quadrupole splitting (mm/s)				
Fe^{2+}	1.92	1.99		1.68
Fe^{2+}*	1.02	1.22		
Magnetic field (kOe)[a]				
Alloy		353	343	336
I	171	170		
II	217			
III	124			
Average outer ferromagnetic linewidth (mm/s)[a]				
Alloy		0.65	0.57	0.53
I	0.41	1.00		
II	0.54			
III	0.35			
Fraction of spectral area magnetically split[a]				
Alloy		0.76	1.00	0.90
I	0.66	0.14		
II	0.07			
III	0.06			

[a] I, II, III are three iron sites in iron carbide.

differentiation is not our objective here, we follow the original asssignment of Hofer, and refer to all the hexagonal and pseudo-hexagonal carbides as ϵ (*47*).

In order to simplify the analysis, the carbide spectra were fit assuming that three different Fe sites are present, as was done by Bernas *et al.* for χ carbide (*43*). The results of fitting spectrum 4A, assuming that 18 peaks for the three different Fe sites are present along with 4 peaks for the unreduced oxide, are listed in Table 3. The unreduced oxide peaks were constrained to be unchanged from the fit of the reduced catalyst. The high relative intensity of site I iron shows that the main constituent in this sample is the carbide with iron at site I only. This is the phase we define as ϵ and the hyperfine field of 170 kOe shown in Table 3 agrees well with the expected value of 173 kOe (*39*). The remaining carbide has low intensity and is thus difficult to fit reliably, but on the basis of the presence of site II and site III iron we assign it as χ carbide. Similar results were obtained by fitting spectra of other samples of the same composition, but the air-dried sample was not completely carbided after 6 hr of reaction.

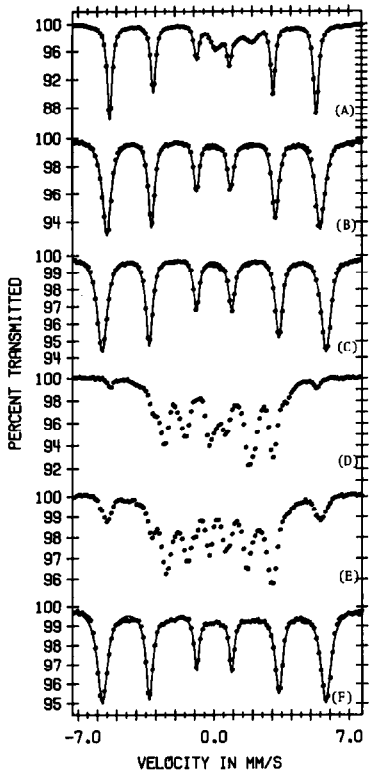

FIG. 5. Room-temperature Mössbauer spectra of reduced and reacted vacuum-dried catalysts. (A) 10Fe/SiO_2, reduced 8 hr; (B) 8.95Fe1.05Co/SiO_2, reduced 8 hr; (C) 7.4Fe2.6Co/SiO_2, reduced 8 hr; (D) 10Fe/SiO_2, reacted 6 hr; (E) 8.95Fe1.05Co/SiO_2, reacted 6 hr; (F) 7.4Fe2.6Co/SiO_2, reacted 6 hr.

Approximately 13% of the spectral area was still metallic. Raupp and Delgass (*48, 49*) found a similar decrease in the rate of carburization with increased particle size for iron catalysts.

Although limited, a detectable amount of carbide formed during reaction for the 7.4Fe2.6Co/SiO_2 catalyst shown in spectrum 4B. Computer analysis of the spectrum revealed that all of the carbide material could be accounted for by one six-line set of peaks. The fitted parameters are listed in Table 3, and these parameters indicate that the carbide phase formed is ϵ carbide.

In order to further examine the effects of Co in the range of composition in which carburization does occur, we prepared three catalysts, 10Fe/SiO_2, 8.95Fe1.05Co/SiO_2, and 7.4Fe2.6Co/SiO_2, by the vacuum-drying technique. The samples were reduced as before, and room-temperature spectra were recorded in H_2. As shown in Figs. 5A–C, increased reducibility, increased magnetic splitting, and increased linewidth accompany Co addition, as expected from our earlier discussion.

These catalysts were subjected to $3.2H_2/CO$ syngas flowing at 20 cm^3/min at 523°K for 6 hr. Spectra 5D–F are for the used catalysts after cooling to room temperature in He. Again, the 7.4 Fe2.6Co/SiO_2 catalyst showed only limited carbide formation, but both of the higher-Fe-content catalysts underwent extensive carburization. The remaining metallic peaks at high and low velocities in Figs. 5D and E show that carburization was not complete after 6 hr of reaction. The 10Fe/SiO_2 catalyst exhibited a higher conversion to carbide than the 8.95Fe1.05Co/SiO_2 sample even though its average particle size was larger (16 vs 13 nm). Since Raupp and Delgass (*48, 49*) have confirmed the expectation that larger particles should carburize slower, spectra 5D and E show that the Co is responsible for a decrease in carburization rate. This finding is no surprise since carburization does not occur at all at the higher Co loadings.

The results of computer fits for spectra 5A–C and F are cited in Table 4. The fit to spectrum 5F was obtained by constraining the magnetic field of the carbide peaks to be 169.9 kOe. The large linewidths for those peaks (6.60 mm/s) show that this species has been forced to account for the bowed background of the spectrum. Thus the fit is not accurate for species identification but does indicate the presence of a second phase. Attempts to fit spectra 5D and E generally suggest the presence of both ϵ (H = 173 kOe) and χ carbides. The accuracy of the fits is in question, however, because the 6 additional peaks from the metal required

TABLE 4

Mössbauer Parameters and Estimated Particle Sizes for Reduced and Reacted Catalysts, Fig. 5

Spectrum:	A	B	C	F
Catalyst:	10Fe/SiO_2	8.95Fe1.05Co/SiO_2	7.4Fe2.6Co/SiO_2	7.4Fe2.6Co/SiO_2
Isomer shift (mm/s)				
Fe or alloy	0.01	0.02	0.04	0.04
Fe^{2+}	1.06			
Fe^{2+*}	0.80			
I				0.28
Quadrupole splitting (mm/s)				
Fe^{2+}	1.90			
Fe^{2+*}	0.98			
Magnetic field (kOe)				
Fe or alloy	331.3	342.2	359.4	358.4
I				169.9
Average outer ferromagnetic linewidth (mm/s)				
Fe or alloy	0.32	0.56	0.60	0.63
I				6.60
Fraction of spectral area magnetically split				
Fe or alloy	0.79	1.00	1.00	0.66
I				0.34
Estimated particle size–XRD (nm)	16	13	12	12

use of as many as 28 peaks. The time requirement for convergence of the fit was huge (1024 s) and even longer times would have been necessary for random steps to be made to check the stability of the point of convergence. To help identify the phases present, *ex situ* XRD was used. This is justified since Mössbauer examination showed that the carbides were stable in air for periods of greater than 4 months.

XRD of 10Fe/SiO_2 and 8.95Fe1.05Co/SiO_2 samples similar to those discussed above showed the major peaks reported by Barton and Gale (d = 2.13 and 2.10 Å) for XRD of a pseudo-hexagonal Fe carbide (*46*) and that reported by Senateur for χ carbide (d = 2.05 Å) (*50*). The carbide we call ϵ was the major component in the X-ray diffraction pattern, in agreement with the Mössbauer results cited in Table 3 for the 9.47Fe0.53Co/SiO_2 catalyst.

Oxidized Catalysts

Figure 6 shows spectra for three different catalyst compositions after vacuum drying, reduction, and subsequent reoxidation in a 21% O_2/79% He gas mixture for 1 hr at 623°K. The spectra are no longer those of simply quadrupole split Fe^{3+}, but now include additional broad, magnetically split peaks. Spectra A, B, and C in Fig. 7 show the corresponding reoxidation of the air-dried catalysts. It is clear from comparing Figs. 6 and 7 that a larger fraction of magnetically split material, and therefore more large oxide crystallites, are present in the air-dried samples. This result is in agreement with our findings for the reduced catalysts.

XRD phase identification and particle size measurements for the oxidized catalysts were attempted, but for the most part failed because of poor peak resolution in

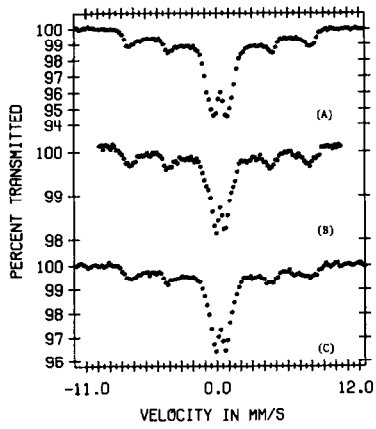

FIG. 6. Room-temperature Mössbauer spectra of vacuum-dried catalysts after reduction and reoxidation at 623°K in a 21% O_2/He mixture for 1 hr. (A) 9.47Fe0.53Co/SiO_2, estimated particle size of reduced alloy crystallites from XRD line broadening is 11 nm; (B) 4.87Fe5.13Co/SiO_2, estimated reduced crystallite size of 12 nm; (C) 3.87Fe6.13Co/SiO_2, estimated reduced crystallite size of 12 nm.

the spectra. Such broad, poorly resolved peaks, usually attributable to particle sizes less than 5 nm, are surprising since in the reduced state the average size was always in excess of 8 nm and the lattice should expand with the incorporation of oxygen. Recently, similar results obtained by Unmuth *et al.* for Fe-on-silica catalysts were explained by the recrystallization of the particles into smaller subdivisions or grains upon oxidation (*51*). The results presented here show that in spite of the reduction in grain size on oxidation, bigger metallic crystallites tend to form more oxide of larger grain size (as shown by the larger fraction of magnetically split material in the Mössbauer spectrum).

The bulk phase diagram for $Co_xFe_{3-x}O_4$ indicates that below 923°K a two-phase solution of hematite (α-Fe_2O_3) and a Co-rich spinel should exist (*52*). On the other hand, small particle sizes and support interactions are known to distort bulk phase diagrams. The magnetically split Mössbauer component suggests the presence of some spinel phase, because α-Fe_2O_3 would be superparamagnetic at the small particle sizes consistent with the XRD patterns.

The Mössbauer spectra of the air-dried samples are better resolved than those of the vacuum-dried material but attempts to fit them with as many as 16 Lorentzian lines failed because of the asymmetry of the peaks. Disorder can broaden the spinel peaks but the asymmetry of the right as well as the left peaks suggests a contribution from the combination of a particle size distribution and collective oscillations of the magnetization (*36*). For the material giving spectrum 7B, the lattice parameter of 8.25 Å calculated from the location of the broad (311) peak agrees with the value reported by Tseung and Goldstein for Co ferrites on the same composition (*53*). Agreement of the Mössbauer hyperfine field with that measured for a $CoFe_2O_4$ sample (Alpha/Ventron) having a sharp XRD pattern characteristic of the ferrites, suggests that oxidation of the FeCo alloy particles forms some $Co_xFe_{3-x}O_4$. The lack of splitting of the left peaks in spectrum 7A, however, suggests that the composition of the

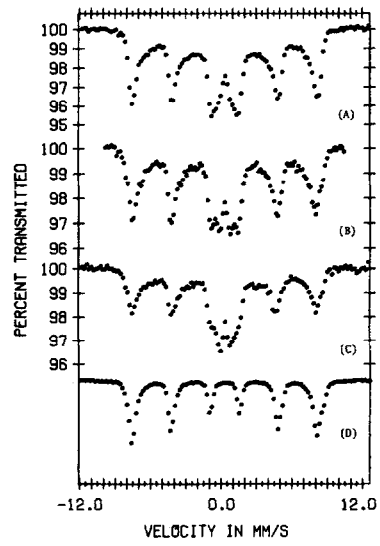

FIG. 7. Room-temperature Mössbauer spectra of air-dried catalysts after reduction and reoxidation at 623°K in a 21% O_2/He mixture for 1 hr. (A) 9.47Fe0.53Co/SiO_2, estimated reduced crystallite size of 21 nm; (B) 4.87Fe5.13Co/SiO_2, estimated reduced crystallite size of 20 nm; (C) 3.87Fe6.13Co/SiO_2, estimated reduced crystallite size of 14 nm; (D) bulk, powdered $CoFe_2O_4$ obtained from Alpha/Ventron.

mixed oxide need not follow that of the alloy.

CONCLUSIONS

The data presented here show that on an appropriate silica support iron and cobalt can form alloy particles with approximately 10 nm diameter and reasonable homogeneity. The alloys are close to the nominal composition but are not ordered. Air drying of the catalysts produces larger metallic crystallites than vacuum drying. The addition of cobalt to iron in this system enhances the reducibility of the iron. At cobalt concentrations in iron above 25%, carburization during Fischer–Tropsch synthesis at 523°K and 3.2 H_2/CO is prevented. Lower cobalt concentrations retard the carburization rate.

It is important to emphasize that the success in alloy formation reported here depends critically on the pore structure of the support and the dehydration procedure before reduction. Rapid removal of water and lack of porosity (present because the Cabo-Sil is a pressed wafer) can restrict agglomeration of the metals and prevent production of alloy particles (*54*).

ACKNOWLEDGMENT

It is a pleasure to acknowledge the National Science Foundation for support of this work through Grants DMR77-23798 and ENG76-20853.

REFERENCES

1. Anderson, R. B., and Hofer, L. J. E., *in* "Catalysis" (P. H. Emmett, Ed.), Vol. IV. Reinhold, New York, 1956.
2. Storch, H. H., Golumbic, H., and Anderson, R. B., "The Fischer-Tropsch and Related Synthesis." Wiley, New York, 1951.
3. Mann, R. S., and Lien, P. C., *J. Catal.* **15,** 1 (1969).
4. Schuit, G. C. A., and vanReijen, L. L., *in* "Advances in Catalysis and Related Subjects," Vol. 10, p. 242. Academic Press, New York/London, 1958.
5. Vannice, M. A., *J. Catal.* **50,** 228 (1977).
6. Vannice, M. A., *J. Catal.* **37,** 447 (1975).
7. Vannice, M. A., and Garten, R. L., *J. Mol. Catal.* **1,** 201 (1975–1976).
8. Pichler, H., *in* "Advances in Catalysis and Related Subjects," Vol. 4, p. 271. Academic Press, New York/London, 1952.
9. Stowe, R. A., and Russell, W. W., *J. Amer. Chem. Soc.*, **76**(2), 319 (1954).
10. Broden, G., Gafner, G., and Bonzel, H. P., *Appl. Phys.* **13,** 333 (1977).
11. Rhodin, T. N., and Brucker, C. F., *Solid State Commun.* **23,** 275 (1977).
12. Textor, M., Gay, I. D., and Mason, R., *Proc. R. Soc. London Ser. A* **356,** 37 (1977).
13. Brundle, C. R., *IBM J. Res. Dev.* **22,** 235 (1978).
14. Bridge, M. E., Comrie, C. M., and Lambert, R. M., *Surf. Sci.* **67,** 393 (1977).
15. Prior, K. A., Schwaha, K., and Lambert, R. M., *Surf. Sci.* **77,** 193 (1978).
16. Pauling, L., *Proc. R. Soc. London Ser. A* **196,** 343 (1949).
17. Pauling, L., "The Nature of the Chemical Bond," 3rd ed. Cornell Univ. Press, Ithaca, N.Y., 1960.
18. (R. Hultgren, Ed.), "Selected Values of the Thermodynamic Properties of Metals and Alloys," Amer. Soc. Metals, Metals Park, Ohio, 1973.
19. Gol'denberg, A. A., and Selisskiy, Ya. P., *Fiz. Met. Metalloved.* **15**(5), 717 (1963).
20. Nakamura, M., Wood, B. J., Hou, P. Y., and Wise H., *in* "Proceedings, 7th International Congress on Catalysis, Tokyo, Japan, June 1980," preprint.
21. Moran-Lopez, J. L., and Wise, H., *Appl. Surf. Sci.* **4**(1), 93 (1980).
22. Kostka, W. D., and Delgass, W. N., to be published.
23. Dumesic, J. A., and Topsøe, H., *in* "Advances in Catalysis and Related Subjects," Vol. 25, p. 121. Academic Press, New York/London, 1976.
24. Delgass, W. N., Haller, G. L., Kellerman, R., and Lunsford, J. H., "Spectroscopy in Heterogeneous Catalysis." Academic Press, New York, 1979.
25. DeMayo, B., Forrestor, D. W., and Spooner, S., *J. Appl. Phys.* **41**(3), 1319 (1970).
26. Vince, I., Campbell, I. A., and Meyer, A. J., *Solid State Commun.* **15,** 1495 (1974).
27. Johnson, C. E., Ridout, M. S., and Cranshaw, T. E., *Proc. Phys. Soc. London* **81,** 1079 (1963).
28. Raupp, G. B., and Delgass, W. N., *J. Catal.* **58,** 337 (1979).
29. Delgass, W. N., Chen, L. Y., and Vogel, G., *Rev. Sci. Instrum.* **47,** 968 (1976).
30. Davidon, W. C., Rep. ANL—5990(Rev 2), Argonne Natl. Lab., Lamont, Ill., 1966.
31. Margulies, S., and Ehrman, J. R., *Nucl. Instrum. Methods* **12,** 131 (1961).
32. Gager, H. M., and Hobson, M. C., Jr., *Catal. Rev. Sci. Eng.* **11**(1), 117 (1975).
33. Garten, R. L., *in* "Mössbauer Effect Methodology" (I. J. Grumerman and C. W. Seidel, Eds.), Vol. 10, p. 69. Plenum, New York, 1976.

34. Vannice, M. A., Lam, Y. L., and Garten, R. L., *Amer. Chem. Soc. Div. Pet. Chem. Prepr.* **23,** 495 (1978).
35. Aschenbeck, D., Ph.D. thesis, Purdue University, 1979.
36. Mørup, S., Topsøe, H., and Lipka, J., *J. Physique* **37,** C6-287 (1976).
37. Kundig, W., Bommel, H., Constabaris, G., and Lindquist, R. H., *Phys. Rev.* **142,** 327 (1966).
38. Ino, H., Moriya, T., Fujita, F. E., Maeda, Y., Ono, Y., and Inokuti, Y., *J. Phys. Soc. Japan* **25,** 88 (1968).
39. Amelse, J. A., Butt, J. B., and Schwartz, L. H., *J. Phys. Chem.* **82,** 558 (1978).
40. Maksimov, Yu. V., Suzdalev, I. P., Arents, R. A., and Loktev, S. M., *Kinet. Katal.* **15,** 1293 (1974).
41. LeCaer, G., Simon, A., Lorenzo, A., and Genin, J. M., *Phys. Status Solidi A* **6,** K97 (1971).
42. Hirotsu, Y., and Nagakura, S., *Acta Metall.* **20,** 645 (1972).
43. Bernas, H., Campbell, I. A., and Fruchart, R., *J. Phys. Chem. Solids* **28,** 17 (1967).
44. Arents, R. A., Maksimov, Yu. V., Suzdalev, I. P., Imshennik, V. K., and Krupyanskiy, Yu. F., *Fiz. Met. Metalloved.* **36,** 277 (1973).
45. Niemantsverdriet, J. W., van der Kraan, A. M., van Dijk, W. L., and van der Baan, H. S., *J. Phys. Chem.* **84,** 3863 (1980).
46. Barton, G. H., and Gale, B., *Acta Crystallogr.* **17,** 1460 (1964).
47. Hofer, L. J. E., *in* "Catalysis" (P. H. Emmett, Ed.), Vol. IV, p. 373. Reinhold, New York, 1956.
48. Raupp, G. B., and Delgass, W. N., *J. Catal.* **58,** 348 (1979).
49. Raupp, G. B., and Delgass, W. N., *J. Catal.* **58,** 361 (1979).
50. Senateur, J. P., *Ann. Chim.* (*Paris*) **2,** 103 (1967).
51. Unmuth, E. E., Schwartz, L. H., and Butt, J. B., *J. Catal.* **61,** 242 (1980).
52. Schwab, G. M. (Ed.), "Reactivity of Solids." p. 597. Elsevier, New York, 1965.
53. Tseung, A. C. C., and Goldstein, J. R., *J. Mater. Sci.* **7,** 1383 (1972).
54. Stanfield, R. M., and Delgass, W. N., to be published.